UWThPh-1996-6
HEPHY-PUB 640/96
hep-ph/9603206

February, 1996

SUSY–QCD corrections to scalar quark pair production in e^+e^- annihilation

H. Eberl[1], A. Bartl[2], W. Majerotto[1]

[1] *Institut für Hochenergiephysik der Österreichischen Akademie der Wissenschaften*
[2] *Institut für Theoretische Physik, Universität Wien, A-1090 Vienna, Austria*

Abstract

We calculate the supersymmetric $\mathcal{O}(\alpha_s)$ QCD corrections to the cross section $e^+e^- \to \tilde{q}_i\bar{\tilde{q}}_j$ $(i,j=1,2)$ within the Minimal Supersymmetric Standard Model. We pay particular attention to the case of the left–right squark mixing and to the renormalization of the mixing angle. The corrections due to gluino exchange turn out to be smaller than those due to gluon exchange, but they can be significant at higher energies even for a gluino mass of a few hundred GeV.

1 Introduction

Supersymmetry [1] requires the existence of two scalar partners $\tilde{q}_L$ and $\tilde{q}_R$ (squarks) for every quark q. Quite generally, $\tilde{q}_L$ and $\tilde{q}_R$ mix, the size of mixing being proportional to the mass of the quark [2]. Therefore, the scalar partners of the top quark are expected to be strongly mixed so that one mass eigenstate $\tilde{t}_1$ can be rather light. Within the Minimal Supersymmetric Standard Model (MSSM) $\tilde{b}_L$ and $\tilde{b}_R$ can considerably mix [3, 4] for large $\tan\beta = v_2/v_1$ (where v_1 and v_2 are the vacuum expectation values of the neutral components of the two Higgs doublets). Therefore, it is possible that $\tilde{t}_1$ or $\tilde{b}_1$ will be discovered in the energy range of the present colliders.

The stop production in e^+e^- annihilation, $e^+e^- \to \tilde{t}_1\bar{\tilde{t}}_1$, was first studied at tree level in [5]. The conventional QCD corrections to this process including virtual and real (soft and hard) gluon radiation were given in [6, 7]. These corrections are quite large, for instance, they are about 35% for $m_{\tilde{t}_1} = 80$ GeV at $\sqrt{s} = 190$ GeV [8]. The QCD corrections within the MSSM including virtual gluino and squark exchange were first calculated in [9], where the process $e^+e^- \to \tilde{q}_1\bar{\tilde{q}}_2$ was also included. However, the renormalization of the squark mixing angle $\theta_{\tilde{q}}$ as adopted there is not applicable in the whole range of $\theta_{\tilde{q}}$ for the diagonal channels $e^+e^- \to \tilde{q}_1\bar{\tilde{q}}_1$, $\tilde{q}_2\bar{\tilde{q}}_2$. A proper renormalization of the squark mixing angle is necessary whenever stop and sbottom play a rôle. Moreover, no numerical analysis at all has been given so far for the unequal mass case or for squark mixing angle $\theta_{\tilde{q}} \neq 0$.

Here we want to present the complete formulae for the supersymmetric QCD corrections up to $\mathcal{O}(\alpha_s)$ within the MSSM including virtual and real gluon exchange, virtual gluinos and squarks for general $\tilde{q}_L$–$\tilde{q}_R$ mixing. In particular, we propose a suitable renormalization of the squark mixing angle. Furthermore, we give a detailed numerical analysis of these corrections.

2 Tree level formulae

The squark mixing of $\tilde{q}_L$ and $\tilde{q}_R$ is expressed by

$$\tilde{q}_1 = \tilde{q}_L \cos\theta_{\tilde{q}} + \tilde{q}_R \sin\theta_{\tilde{q}} \quad , \qquad \tilde{q}_2 = -\tilde{q}_L \sin\theta_{\tilde{q}} + \tilde{q}_R \cos\theta_{\tilde{q}} \, , \tag{1}$$

where $\tilde{q}_1$, $\tilde{q}_2$ are the mass eigenstates (with $m_{\tilde{q}_1} < m_{\tilde{q}_2}$) and $\theta_{\tilde{q}}$ is the squark mixing angle. The production $e^+e^- \to \tilde{q}_i\bar{\tilde{q}}_j$, $(i,j = 1,2)$, proceeds via γ and Z exchange in the s–channel (see Fig. 1a), $s = (k+\bar{k})^2$, k and $\bar{k}$ being the four–momenta of the outgoing $\tilde{q}_i$ and $\bar{\tilde{q}}_j$.
The cross section at tree–level is given by:

$$\sigma^0(e^+e^- \to \tilde{q}_i\bar{\tilde{q}}_j) = c_{ij} \left[e_q^2 \delta_{ij} - T_{\gamma Z} e_q a_{ij} \delta_{ij} + T_{ZZ} a_{ij}^2 \right] , \tag{2}$$

with

$$c_{ij} = \frac{\pi\alpha^2}{s} \lambda_{ij}^{3/2} \, , \tag{3}$$

$$T_{\gamma Z} = \frac{v_e}{8 c_W^2 s_W^2} \frac{s(s-m_Z^2)}{(s-m_Z^2)^2 + \Gamma_Z^2 m_Z^2} \, , \tag{4}$$

$$T_{ZZ} = \frac{(a_e^2 + v_e^2)}{256 s_W^4 c_W^4} \frac{s^2}{(s-m_Z^2)^2 + \Gamma_Z^2 m_Z^2} \, . \tag{5}$$

Here $\lambda_{ij} = (1 - \mu_i^2 - \mu_j^2)^2 - 4\mu_i^2\mu_j^2, \mu_{i,j}^2 = m_{\tilde{q}_{i,j}}^2/s$; e_q is the charge of the squarks ($e_t = 2/3, e_b = -1/3$) in units of $e(=\sqrt{4\pi\alpha})$. a_e and v_e are the vector and axial vector couplings of the electron to the Z boson: $v_e = -1 + 4s_W^2$ (with $s_W \equiv \sin\theta_W$), $a_e = -1$, and a_{ij} are the corresponding couplings $Z\tilde{q}_i\bar{\tilde{q}}_j$:

$$a_{11} = 4(I_q^{3L} \cos^2\theta_{\tilde{q}} - s_W^2 e_q) \ , \ a_{22} = 4(I_q^{3L} \sin^2\theta_{\tilde{q}} - s_W^2 e_q) \ , \ a_{12} = a_{21} = -2 I_q^{3L} \sin 2\theta_{\tilde{q}} \, , \tag{6}$$

where I_q^{3L} is the third component of the weak isospin of the quark q.

3 SUSY–QCD corrections

The supersymmetric QCD corrected cross section in $\mathcal{O}(\alpha_s)$ corresponding to the Fig. 1 can be written as:

$$\sigma = \sigma^0 + \delta\sigma^g + \delta\sigma^{\tilde{g}} + \delta\sigma^{\tilde{q}} \, . \tag{7}$$

$\delta\sigma^g$ gives the standard QCD gluonic correction (Figs. 1b–f), $\delta\sigma^{\tilde{g}}$ is the correction due to the gluino exchange (Figs. 1g, 1h) and $\delta\sigma^{\tilde{q}}$ due to the squark exchange (Figs. 1i, 1j). As will be seen later, within the renormalization prescription used $\delta\sigma^{\tilde{q}} = 0$.

According to eq. (2) the correction can be written as:

$$\delta\sigma^a = c_{ij}\left[2e_q\Delta(e_q)_{ij}^{(a)}\delta_{ij} - T_{\gamma Z}(e_q\delta_{ij}\Delta a_{ij}^{(a)} + \Delta(e_q)_{ij}^{(a)}a_{ij}) + 2T_{ZZ}a_{ij}\Delta a_{ij}^{(a)}\right] \quad , a = g, \tilde{g}, \tilde{q}\,. \quad (8)$$

3.1 Gluonic correction

$\delta\sigma^g$ can be written as

$$\delta\sigma^g = \sigma^0\left[\frac{4}{3}\frac{\alpha_s}{\pi}\Delta_{ij}\right]. \quad (9)$$

Δ_{ij} has the following expression:

$$\begin{aligned}
\Delta_{ij} &= \log(\mu_i\mu_j) + 2 + \frac{2+\mu_i^2+\mu_j^2}{\lambda_{ij}^{1/2}}\log\lambda_0 + \frac{1+2\mu_i^2}{\lambda_{ij}^{1/2}}\log\lambda_1 + \frac{1+2\mu_j^2}{\lambda_{ij}^{1/2}}\log\lambda_2 \\
&+ \frac{1-\mu_i^2-\mu_j^2}{\lambda_{ij}^{1/2}}\log\frac{1-\mu_i^2-\mu_j^2+\lambda_{ij}^{1/2}}{1-\mu_i^2-\mu_j^2-\lambda_{ij}^{1/2}} + \left[\frac{(1-\mu_i^2-\mu_j^2)}{\lambda_{ij}^{1/2}}\log\lambda_0 - 1\right]\log\frac{\lambda_{ij}^2}{\mu_i^2\mu_j^2} \quad (10) \\
&+ \frac{4}{\lambda_{ij}^{3/2}}\left[\frac{1}{4}\lambda_{ij}^{1/2}(1+\mu_i^2+\mu_j^2) + \mu_i^2\log\lambda_2 + \mu_j^2\log\lambda_1 + \mu_i^2\mu_j^2\log\lambda_0\right] + \frac{1-\mu_i^2-\mu_j^2}{\lambda_{ij}^{1/2}}\left[\frac{2\pi^2}{3}\right. \\
&+ \left. 2\mathrm{Li}_2(1-\lambda_0^2) + \mathrm{Li}_2(\lambda_1^2) - \mathrm{Li}_2(1-\lambda_1^2) + \mathrm{Li}_2(\lambda_2^2) - \mathrm{Li}_2(1-\lambda_2^2) + 2\log^2\lambda_0 - \log\lambda_{ij}\log\lambda_0\right],
\end{aligned}$$

with

$$\lambda_0 = \frac{1}{2\mu_i\mu_j}(1-\mu_i^2-\mu_j^2+\lambda_{ij}^{1/2}) \quad , \quad \lambda_{1,2} = \frac{1}{2\mu_{j,i}}(1\mp\mu_i^2\pm\mu_j^2-\lambda_{ij}^{1/2})\,, \quad (11)$$

and $\mathrm{Li}_2(x) = -\int_0^1 \log(1-xt)/t\,\mathrm{d}t$. Eq. (10) has been calculated from the graphs in Figs. 1b–f including soft and hard gluon radiation. For $i = j$ the expression eq. (10) was already derived in [6, 7, 9, 10]. For $i \neq j$ we also agree with the calculation of ref. [9] apart from an obvious misprint in eq. (3.2) of [9].

3.2 The four–squark interaction

Quite generally, we can decompose the corrections due to the four–squark interaction (Figs. 1i, 1j) in the following way:

$$\Delta a_{ij}^{(\tilde{q})} = \delta a_{ij}^{(v,\tilde{q})} + \delta a_{ij}^{(w,\tilde{q})} + \delta a_{ij}^{(\tilde{\theta},\tilde{q})} , \tag{12}$$

$$\Delta (e_q)_{ij}^{(\tilde{q})} = \delta (e_q)_{ij}^{(v,\tilde{q})} + \delta (e_q)_{ij}^{(w,\tilde{q})} . \tag{13}$$

Here the upper index v denotes the vertex correction (Fig. 1i), w the wave–function correction (Fig. 1j), and $\tilde{\theta}$ the renormalization of the mixing angle $\theta_{\tilde{q}}$. The last term in eq. (12) is necessary as the couplings a_{ij} depend on the mixing angle (see eq. (6)). The vertex correction is proportional to the momentum of the exchanged photon or Z boson, and hence the related matrix element for $e^+e^- \to \tilde{q}_i \bar{\tilde{q}}_j$ is zero, that is $\delta a_{ij}^{(v,\tilde{q})} = \delta (e_q)_{ij}^{(v,\tilde{q})} = 0$. There is, however, a squark wave–function correction $\delta a_{ij}^{(w,\tilde{q})}$ due to the four–squark interaction.
The self–energies due to the squark loops in Fig. 1j are given by:

$$\Sigma_{ij}^{(\tilde{q})}(p^2) = \frac{1}{3}\frac{\alpha_s}{\pi} \begin{pmatrix} \cos^2 2\theta_{\tilde{q}} A^0(m^2_{\tilde{q}_1}) + \sin^2 2\theta_{\tilde{q}} A^0(m^2_{\tilde{q}_2}) & \frac{1}{2}\sin 4\theta_{\tilde{q}} \left(A^0(m^2_{\tilde{q}_2}) - A^0(m^2_{\tilde{q}_1}) \right) \\ \frac{1}{2}\sin 4\theta_{\tilde{q}} \left(A^0(m^2_{\tilde{q}_2}) - A^0(m^2_{\tilde{q}_1}) \right) & \sin^2 2\theta_{\tilde{q}} A^0(m^2_{\tilde{q}_1}) + \cos^2 2\theta_{\tilde{q}} A^0(m^2_{\tilde{q}_2}) \end{pmatrix} . \tag{14}$$

Here A^0 is the standard one–point function [11], $A^0(m^2) = -i\pi^{-2} \int d^D q (q^2 - m^2)^{-1}$ in the convention of [12]. Notice that the self–energies are independent of p^2, hence $\Sigma_{ij}^{(\tilde{q})}(m^2_{\tilde{q}_1}) = \Sigma_{ij}^{(\tilde{q})}(m^2_{\tilde{q}_2}) = \Sigma_{ij}^{(\tilde{q})}$. We therefore get for $\delta a_{ij}^{(w,\tilde{q})}$:

$$\delta a_{ij}^{(w,\tilde{q})} = \delta Z_{i'i}^{(\tilde{q})} a_{i'j} + \delta Z_{j'j}^{(\tilde{q})} a_{ij'} = -\mathrm{Re} \left\{ \frac{\Sigma_{i'i}^{(\tilde{q})}}{m^2_{\tilde{q}_i} - m^2_{\tilde{q}_{i'}}} a_{i'j} + \frac{\Sigma_{j'j}^{(\tilde{q})}}{m^2_{\tilde{q}_j} - m^2_{\tilde{q}_{j'}}} a_{ij'} \right\} , \begin{array}{c} i \neq i' \\ j \neq j' \end{array} , \tag{15}$$

with the squark wave–function renormalization constants

$$\delta Z_{12}^{(\tilde{q})} = \frac{\mathrm{Re}\left\{\Sigma_{12}^{(\tilde{q})}\right\}}{m^2_{\tilde{q}_1} - m^2_{\tilde{q}_2}} \quad , \quad \delta Z_{21}^{(\tilde{q})} = \frac{\mathrm{Re}\left\{\Sigma_{21}^{(\tilde{q})}\right\}}{m^2_{\tilde{q}_2} - m^2_{\tilde{q}_1}} . \tag{16}$$

Note that $\delta (e_q)_{ij}^{(w,\tilde{q})} = 0$ because the contributions coming from the squark loop Fig. 1j and the corresponding graph with the loop at the antisquark cancel each other. Hence $\Delta (e_q)_{ij}^{(\tilde{q})} = 0$. The correction term $\delta a_{ij}^{(\tilde{\theta},\tilde{q})}$ in eq. (12) will be treated in section 3.4.

3.3 Correction due to gluino exchange

Now we turn to the corrections due to gluino exchange (Fig. 1g, 1h). As in eq. (12) and eq. (13) we can write:

$$\Delta a_{ij}^{(\tilde{g})} = \delta a_{ij}^{(v,\tilde{g})} + \delta a_{ij}^{(w,\tilde{g})} + \delta a_{ij}^{(\tilde{\theta},\tilde{g})} , \tag{17}$$

$$\Delta (e_q)_{ij}^{(\tilde{g})} = \delta (e_q)_{ij}^{(v,\tilde{g})} + \delta (e_q)_{ij}^{(w,\tilde{g})} , \tag{18}$$

with $\delta a_{ij}^{(v,\tilde{g})}, \delta (e_q)_{ij}^{(v,\tilde{g})}$ corresponding to the vertex correction (Fig. 1g), and $\delta a_{ij}^{(w,\tilde{g})}, \delta (e_q)_{ij}^{(w,\tilde{g})}$ corresponding to the wave–function correction (Fig. 1h). Again $\delta a_{ij}^{(\tilde{\theta},\tilde{g})}$ is due to the renormalization of the mixing angle and will be calculated in section 3.4.

The gluino vertex corrections are given by:

$$\begin{aligned} \delta a_{ij}^{(v,\tilde{g})} = & \frac{2}{3}\frac{\alpha_s}{\pi} \{ \, 2 m_{\tilde{g}} m_q v_q (S^{\tilde{q}})_{ij} (2 C_{ij}^{+} + C_{ij}^{0}) \\ & + v_q \delta_{ij} \left[(2 m_{\tilde{g}}^2 + 2 m_q^2 + m_{\tilde{q}_i}^2 + m_{\tilde{q}_j}^2) C_{ij}^{+} + 2 m_{\tilde{g}}^2 C_{ij}^{0} + B^0(s, m_q^2, m_q^2) \right] + a_q (A^{\tilde{q}})_{ij} \, [\\ & (2 m_{\tilde{g}}^2 - 2 m_q^2 + m_{\tilde{q}_i}^2 + m_{\tilde{q}_j}^2) C_{ij}^{+} + (m_{\tilde{q}_i}^2 - m_{\tilde{q}_j}^2) C_{ij}^{-} + 2 m_{\tilde{g}}^2 C_{ij}^{0} + B^0(s, m_q^2, m_q^2) \right] \} \, , \end{aligned} \tag{19}$$

and

$$\begin{aligned} \delta (e_q)_{ij}^{(v,\tilde{g})} = & e_q \frac{2}{3}\frac{\alpha_s}{\pi} \{ \, 2 m_{\tilde{g}} m_q (S^{\tilde{q}})_{ij} (2 C_{ij}^{+} + C_{ij}^{0}) \\ & + \delta_{ij} \left[(2 m_{\tilde{g}}^2 + 2 m_q^2 + m_{\tilde{q}_i}^2 + m_{\tilde{q}_j}^2) C_{ij}^{+} + 2 m_{\tilde{g}} C_{ij}^{0} + B^0(s, m_q^2, m_q^2) \right] \} \, , \end{aligned} \tag{20}$$

where δ_{ij} is the identity matrix, $v_q = 2 I_q^{3L} - 4 s_W^2 e_q$, $a_q = 2 I_q^{3L}$,

$$A^{\tilde{q}} = \begin{pmatrix} \cos 2\theta_{\tilde{q}} & -\sin 2\theta_{\tilde{q}} \\ -\sin 2\theta_{\tilde{q}} & -\cos 2\theta_{\tilde{q}} \end{pmatrix} \quad , \quad S^{\tilde{q}} = \begin{pmatrix} -\sin 2\theta_{\tilde{q}} & -\cos 2\theta_{\tilde{q}} \\ -\cos 2\theta_{\tilde{q}} & \sin 2\theta_{\tilde{q}} \end{pmatrix} . \tag{21}$$

The functions $C_{ij}^{\pm}$ are defined by

$$C^{+} = \frac{C^1 + C^2}{2} \qquad , \qquad C^{-} = \frac{C^1 - C^2}{2} . \tag{22}$$

The arguments of all C–functions are $(m_{\tilde{q}_i}^2, s, m_{\tilde{q}_j}^2, m_{\tilde{g}}^2, m_q^2, m_q^2)$. B^0, C^0, C^1, and C^2 are the usual two– and three–point functions as given, for instance, in [12]:

$$\begin{aligned} B^0(k^2, m_1^2, m_2^2) &= \int \frac{d^D q}{i\pi^2} \frac{1}{(q^2 - m_1^2)((q+k)^2 - m_2^2)} , \\ \left[C^0, k^\mu C^1 - \bar{k}^\mu C^2 \right] &= \int \frac{d^D q}{i\pi^2} \frac{[1, q^\mu]}{(q^2 - m_{\tilde{g}}^2)((q+k)^2 - m_q^2)((q-\bar{k})^2 - m_q^2)} . \end{aligned}$$

The squark wave–function renormalization due to the squark self–energy graphs with gluino exchange (Fig. 1h) leads in the on–shell scheme to:

$$\begin{aligned}\delta a_{ij}^{(w,\tilde{g})} &= \frac{1}{2}(\delta Z_{ii}^{(\tilde{g})} + \delta Z_{jj}^{(\tilde{g})})a_{ij} + \delta Z_{i'i}^{(\tilde{g})} a_{i'j} + \delta Z_{j'j}^{(\tilde{g})} a_{ij'} \qquad (23)\\ &= -\mathrm{Re}\left\{ \frac{1}{2}\left[\Sigma_{ii}^{\prime(\tilde{g})}(m^2_{\tilde{q}_i}) + \Sigma_{jj}^{\prime(\tilde{g})}(m^2_{\tilde{q}_j})\right] a_{ij} + \frac{\Sigma_{i'i}^{(\tilde{g})}(m^2_{\tilde{q}_i})}{m^2_{\tilde{q}_i} - m^2_{\tilde{q}_{i'}}} a_{i'j} + \frac{\Sigma_{j'j}^{(\tilde{g})}(m^2_{\tilde{q}_j})}{m^2_{\tilde{q}_j} - m^2_{\tilde{q}_{j'}}} a_{ij'} \right\}, \begin{array}{c} i \neq i' \\ j \neq j' \end{array},\end{aligned}$$

and

$$\delta(e_q)_{ii}^{(w,\tilde{g})} = -e_q \mathrm{Re}\left\{\Sigma_{ii}^{\prime(\tilde{g})}(m^2_{\tilde{q}_i})\right\}, \quad \delta(e_q)_{12}^{(w,\tilde{g})} = \frac{e_q}{m^2_{\tilde{q}_1} - m^2_{\tilde{q}_2}} \mathrm{Re}\left\{\Sigma_{12}^{(\tilde{g})}(m^2_{\tilde{q}_2}) - \Sigma_{21}^{(\tilde{g})}(m^2_{\tilde{q}_1})\right\}, \quad (24)$$

with the squark self–energy contributions $\Sigma_{ij}^{(\tilde{g})}(m^2)$ and their derivatives $\Sigma_{ii}^{\prime(\tilde{g})}(m^2) = \partial\Sigma_{ii}^{(\tilde{g})}(p^2)/\partial p^2|_{p^2=m^2}$:

$$\Sigma_{12}^{(\tilde{g})}(p^2) = \Sigma_{21}^{(\tilde{g})}(p^2) = \frac{4}{3}\frac{\alpha_s}{\pi} m_{\tilde{g}} m_q \cos 2\theta_{\tilde{q}} B_0(p^2, m^2_{\tilde{g}}, m^2_q) \qquad (25)$$

and

$$\begin{aligned}\Sigma_{ii}^{\prime(\tilde{g})}(p^2) &= \frac{2}{3}\frac{\alpha_s}{\pi}\Big[B_0(p^2, m^2_{\tilde{g}}, m^2_q) + (p^2 - m^2_q - m^2_{\tilde{g}}) B_0'(p^2, m^2_{\tilde{g}}, m^2_q)\\ &\qquad -2m_q m_{\tilde{g}} (-1)^i \sin 2\theta_{\tilde{q}} B_0'(p^2, m^2_{\tilde{g}}, m^2_q)\Big]. \qquad (26)\end{aligned}$$

3.4 The renormalization of the squark mixing angle

We still have to discuss the renormalization of the squark mixing angle $\delta a_{ij}^{(\tilde{\theta},\tilde{q})}$, eq. (12), and $\delta a_{ij}^{(\tilde{\theta},\tilde{g})}$, eq. (17). From eq. (6) one gets for $\delta a_{ij}^{(\tilde{\theta},a)}$ (with $a = \tilde{q}, \tilde{g}$):

$$\delta a_{11}^{(\tilde{\theta},a)} = 2a_{12}\delta\theta_{\tilde{q}}{}^{(a)} = -\delta a_{22}^{(\tilde{\theta},a)} \qquad \delta a_{12}^{(\tilde{\theta},a)} = \delta a_{21}^{(\tilde{\theta},a)} = (a_{22} - a_{11})\delta\theta_{\tilde{q}}{}^{(a)}. \qquad (27)$$

Now $\Delta a_{ij}^{(\tilde{q})}$ of eq. (12) has to be free from ultra–violet divergencies and is therefore finite. Choosing $\Delta a_{12}^{(\tilde{q})} = 0$ one gets from eqs. (12) and (15)

$$\delta a_{12}^{(\tilde{\theta},\tilde{q})} = (a_{22} - a_{11})\delta\theta_{\tilde{q}}{}^{(\tilde{q})} = -\delta Z_{21}^{(\tilde{q})} a_{22} - \delta Z_{12}^{(\tilde{q})} a_{11}. \qquad (28)$$

Eq. (28) means that the related counterterm $\delta a_{12}^{(\tilde{\theta},\tilde{q})}$ is nothing else than the negative sum of the graphs corresponding to Fig. 1j containing the self–energies $\Sigma_{12}^{(\tilde{q})}$ and $\Sigma_{21}^{(\tilde{q})}$. We now do the

same for $\delta a_{ij}^{(\tilde{\theta},\tilde{g})}$ by taking again the negative sum of those parts of the graphs Fig. 1h, which contain the self–energies $\Sigma_{12}^{(\tilde{g})}(m^2_{\tilde{q}_2})$ and $\Sigma_{21}^{(\tilde{g})}(m^2_{\tilde{q}_1})$. $\delta a_{12}^{(\tilde{\theta},\tilde{g})}$ is then also given by

$$\delta a_{12}^{(\tilde{\theta},\tilde{g})} = (a_{22} - a_{11})\delta\theta_{\tilde{q}}{}^{(\tilde{g})} = -\delta Z_{21}^{(\tilde{g})} a_{22} - \delta Z_{12}^{(\tilde{g})} a_{11}\,, \tag{29}$$

with

$$\delta Z_{12}^{(\tilde{g})} = \frac{\mathrm{Re}\left\{\Sigma_{12}^{(\tilde{g})}(m^2_{\tilde{q}_2})\right\}}{m^2_{\tilde{q}_1} - m^2_{\tilde{q}_2}} \quad , \quad \delta Z_{21}^{(\tilde{g})} = \frac{\mathrm{Re}\left\{\Sigma_{21}^{(\tilde{g})}(m^2_{\tilde{q}_1})\right\}}{m^2_{\tilde{q}_2} - m^2_{\tilde{q}_1}}\,. \tag{30}$$

Inserting the results for $\delta Z_{12}^{(\tilde{q})}, \delta Z_{21}^{(\tilde{q})}$ in eq. (28) and $\delta Z_{12}^{(\tilde{g})}, \delta Z_{21}^{(\tilde{g})}$ in eq. (29), one gets

$$\delta\theta_{\tilde{q}}{}^{(\tilde{q})} = \frac{1}{6}\frac{\alpha_s}{\pi}\frac{\sin 4\theta_{\tilde{q}}}{m^2_{\tilde{q}_1} - m^2_{\tilde{q}_2}}\left(A^0(m^2_{\tilde{q}_2}) - A^0(m^2_{\tilde{q}_1})\right)\,, \tag{31}$$

and

$$\delta\theta_{\tilde{q}}^{(\tilde{g})} = \frac{1}{3}\frac{\alpha_s}{\pi}\frac{m_{\tilde{g}} m_q}{I_q^{3L}(m^2_{\tilde{q}_1} - m^2_{\tilde{q}_2})}\left(B^0(m^2_{\tilde{q}_2}, m^2_{\tilde{g}}, m^2_q)a_{11} - B^0(m^2_{\tilde{q}_1}, m^2_{\tilde{g}}, m^2_q)a_{22}\right)\,. \tag{32}$$

By eqs. (27) we then obtain $\delta a_{ij}^{(\tilde{\theta},\tilde{q})}$ and $\delta a_{ij}^{(\tilde{\theta},\tilde{g})}$. With this result for $\delta a_{ij}^{(\tilde{\theta},\tilde{q})}$ there is no correction from the four–squark interaction graphs: $\Delta a_{ij}^{(\tilde{q})} = 0$, and due to $\Delta(e_q)_{ij}^{(\tilde{q})} = 0$ also $\delta\sigma^{\tilde{q}} = 0$.
By knowing $\delta a_{ij}^{(\tilde{\theta},\tilde{g})}$ we can write the final result for the total gluino correction:

$$\begin{aligned}\Delta a_{ij}^{(\tilde{g})} &= \delta a_{ij}^{(v,\tilde{g})} - \mathrm{Re}\,\{\,\frac{1}{2}\left(\Sigma'_{ii}(m^2_{\tilde{q}_i}) + \Sigma'_{jj}(m^2_{\tilde{q}_j})\right)a_{ij} + \frac{4}{3}\frac{\alpha_s}{\pi}\frac{m_{\tilde{g}} m_q}{m_{\tilde{q}_1} - m_{\tilde{q}_2}}\delta_{ij} \\ &\times \left[B^0(m^2_{\tilde{q}_i}, m^2_{\tilde{g}}, m^2_q)((-1)^{i+1}2a_{ii'}\cos 2\theta_{\tilde{q}} - a_{i'i'}\sin 2\theta_{\tilde{q}}) + B^0(m^2_{\tilde{q}_{i'}}, m^2_{\tilde{g}}, m^2_q)a_{ii}\sin 2\theta_{\tilde{q}}\right]\,\}\,,\end{aligned} \tag{33}$$

with $i' \neq i$, and $\Delta(e_q)_{ij}^{(\tilde{g})} = \delta(e_q)_{ij}^{(v,\tilde{g})} + \delta(e_q)_{ij}^{(w,\tilde{g})}$ as in eq. (18), where $\delta a_{ij}^{(v,\tilde{g})}, \Sigma'_{ii}(m^2_{\tilde{q}_i}), \delta(e_q)_{ij}^{(v,\tilde{g})}$, and $\delta(e_q)_{ij}^{(w,\tilde{g})}$ are given by eqs. (19), (26), (20), and (24), respectively. Note that $\Delta a_{ij}^{(\tilde{g})}$ and $\Delta(e_q)_{ij}^{(\tilde{g})}$ are ultra–violet finite.
Inserting $\Delta a_{ij}^{(\tilde{g})}$ and $\Delta(e_q)_{ij}^{(\tilde{g})}$ in eq. (8) gives the total gluino correction $\delta\sigma^{\tilde{g}}$ which does not factorize as the gluon correction in eq. (9).

Our renormalization condition for the mixing angle $\theta_{\tilde{q}}$ is different from that of [9]. For $\theta_{\tilde{q}} = 0$ and $m_{\tilde{q}_i} = m_{\tilde{q}_j}$ our results agree with those of [9]. However, in the scheme of [9] there appears a singularity at $\theta_{\tilde{q}} = 45^\circ$ going with $\sim \tan 2\theta_{\tilde{q}}$ in the diagonal channels $e^+e^- \to \tilde{q}_1\bar{\tilde{q}}_1$, $\tilde{q}_2\bar{\tilde{q}}_2$, so that this renormalization scheme is numerically not applicable in the region around $\theta_{\tilde{q}} = 45^\circ$. In our scheme there is no such singularity as can be seen in eq. (32) so that it can be applied in the whole range of $\theta_{\tilde{q}}$.

4 Numerical results

We now turn to the numerical analysis of the SUSY–QCD corrections. For the gluonic correction $\delta\sigma^g$ we evaluate eqs. (9), (10) and (11), and for the correction due to gluino exchange $\delta\sigma^{\tilde{g}}$ we take eqs. (33) and (18) together with eq. (8). In the following we have always taken $m_t = 175$ GeV.

We have first calculated the corrections to the cross section $\sigma(e^+e^- \to \tilde{t}_1\bar{\tilde{t}}_1)$ at the LEP2 energy $\sqrt{s} = 190$ GeV as a function of the stop mass $m_{\tilde{t}_1}$ for $\cos\theta_{\tilde{t}} = 0.7$, taking $m_{\tilde{g}} = 200$ GeV and $m_{\tilde{t}_2} = 250$ GeV. This is shown in Fig. 2. The gluon correction is rising from 17% of σ^{tree} for $m_{\tilde{t}_1} = 45$ GeV up to 35% for $m_{\tilde{t}_1} = 80$ GeV. The gluino correction is only about 1% and quite independent of $m_{\tilde{t}_1}$.

In Fig. 3a we show the corrections to the cross section $\sigma(e^+e^- \to \tilde{t}_1\bar{\tilde{t}}_1)$ as a function of the mixing angle $\cos\theta_{\tilde{t}}$, for $\sqrt{s} = 500$ GeV, $m_{\tilde{t}_1} = 150$ GeV, $m_{\tilde{t}_2} = 300$ GeV, and $m_{\tilde{g}} = 300$ GeV. According to eqs. (9) and (10) $\delta\sigma^g$ has the same dependence on $\cos\theta_{\tilde{t}}$ as the tree–level cross section, whereas the gluino correction (see eqs. (33)) introduces a different $\theta_{\tilde{t}}$ dependence. This is due to the fact that the gluino couples equally to $\tilde{t}^*_L t_L$ and to $\tilde{t}^*_R t_R$ and therefore, in the case of mixing, the couplings $\tilde{g}\tilde{t}^*_i t$ get a dependence on the mixing angle $\theta_{\tilde{t}}$. For the c. m. energy and masses chosen the gluino correction is now higher than at LEP2 energies and is about 15% of the gluon correction. Fig. 3b exhibits the $\sqrt{s}$ dependence of $\delta\sigma^g/\sigma^{tree}$ and $\delta\sigma^{\tilde{g}}/\sigma^{tree}$ for $\cos\theta_{\tilde{t}} = 0.7$ and keeping the masses as in Fig. 3a. Notice that $\delta\sigma^g/\sigma^{tree}$ is decreasing with $\sqrt{s}$, whereas $\delta\sigma^{\tilde{g}}/\sigma^{tree}$ is becoming negative at $\sqrt{s} = 700$ GeV with the absolute value increasing with $\sqrt{s}$.
Moreover, we have examined the dependences of $\delta\sigma^{\tilde{g}}/\sigma^{tree}$ in $e^+e^- \to \tilde{t}_1\bar{\tilde{t}}_1$ at fixed $\sqrt{s}$ on the squark masses $m_{\tilde{t}_1}$, $m_{\tilde{t}_2}$, and on their difference. These dependences are weak.

Fig. 4a and b show the $\cos\theta_{\tilde{t}}$ dependence for a higher energy and mass scenario, $\sqrt{s} = 2$ TeV, $m_{\tilde{t}_1} = 500$ GeV, $m_{\tilde{t}_2} = 700$ GeV, and $m_{\tilde{g}} = 600$ GeV. Here $\delta\sigma^{\tilde{g}}$ is about -35% of $\delta\sigma^g$ for $\tilde{t}_1\bar{\tilde{t}}_1$

production. Fig. 4b exhibits the $\tilde{t}_1\bar{\tilde{t}}_2$ channel. $\delta\sigma^g/\sigma^{tree}$ is about 16%. $\delta\sigma^{\tilde{g}}$ is about -40% of $\delta\sigma^g$ at the peak values Notice that the gluino correction is not always positive. In Fig. 4c we also show for this scenario the corrections in the case of the $\tilde{t}_2\bar{\tilde{t}}_2$ production. Here the gluino part is even larger (-50% of the gluon contribution).

We have also computed the SUSY–QCD corrections to $\sigma(e^+e^- \to \tilde{b}_1\bar{\tilde{b}}_1)$. For $\sqrt{s} = 2$ TeV, $m_{\tilde{b}_1} = 500$ GeV, $m_{\tilde{b}_2} = 700$ GeV, and $m_{\tilde{g}} = 600$ GeV $\delta\sigma^{\tilde{g}}$ is about -30% of $\delta\sigma^g$ almost independent of $\cos\theta_{\tilde{b}}$. The gluon correction for $\tilde{b}_i\bar{\tilde{b}}_j$ must be the same as that for $\tilde{t}_i\bar{\tilde{t}}_j$ production, provided the squark masses are the same. This can also be seen explicitely in eq. (10).

It is particularly interesting to study the dependence on the gluino mass. This can be seen in Fig. 5, where we have $\sqrt{s} = 500$ GeV, $m_{\tilde{t}_1} = 150$ GeV, $m_{\tilde{t}_2} = 300$ GeV, and $\cos\theta_{\tilde{t}} = 0.5$ in Fig. 5a, and $\sqrt{s} = 2$ TeV, $m_{\tilde{t}_1} = 500$ GeV, $m_{\tilde{t}_2} = 700$ GeV, and $\cos\theta_{\tilde{t}} = 0.5$ in Fig. 5b. It is somewhat surprising that the gluino correction is first increasing as a function of the gluino mass and only very slowly decreasing. Of course the correction would be largest for a small gluino mass ($m_{\tilde{g}} \lesssim 50$ GeV) but this is excluded by experiment ($m_{\tilde{g}} \gtrsim 130$ GeV).
Here we also want to notice that threshold singularities appear when $m_{\tilde{t}_i} = m_t + m_{\tilde{g}}$. For instance, such a singularity could appear in Fig. 5b for $m_{\tilde{g}} = 325$ GeV. These singularities stem from the self–energy functions in the wave–function renormalization of the stops. This is a known effect and has been also observed in other cases [13].

In conclusion, our analysis of the SUSY–QCD corrections to scalar quark pair production in e^+e^- annihilation has shown that the correction due to the gluino exchange are smaller than the conventional QCD corrections, but they are significant at energies envisaged for the next linear collider [14]. In particular, they exhibit a dependence on the mixing angle $\theta_{\tilde{q}}$, which is different from the tree–level cross section corrected by the gluon exchange. Moreover, the correction due to gluino exchange decreases only very slowly with increasing gluino mass.

Acknowledgements

This work grew out of the Workshop on Physics at LEP2, CERN, 1995, and the Workshop on Physics with e^+e^- Linear Colliders, Annecy – Gran Sasso – Hamburg, 1995. We thank the members of the "Supersymmetry Working Groups" for discussions. This work was supported by the "Fonds zur Förderung der wissenschaftlichen Forschung" of Austria, project no. P10843–PHY.

References

[1] H. E. Haber and G. L. Kane, Phys. Rep. 117 (1985) 75.

[2] J. Ellis and S. Rudaz, Phys. Lett. B128 (1983) 248;
J. F. Gunion, H. E. Haber, Nucl. Phys. B272 (1986) 1.

[3] A. Bartl, W. Majerotto, W. Porod, Z. Phys. C64 (1994) 499.

[4] M. Drees and M. M. Nojiri, Nucl. Phys. B369 (1992) 54.

[5] K. Hikasa and M. Kobayashi, Phys. Rev. D36 (1987) 724.

[6] M. Drees and K. Hikasa, Phys. Lett. B252 (1990) 127.

[7] W. Beenakker, R. Höpker, P. M. Zerwas, Phys. Lett. B349 (1995) 463.

[8] Contribution of the SUSY and New Particles Working Group, conveners: G. Giudice, M. Mangano, G. Ridolfi, R. Rückl, Workshop on Physics at LEP2, CERN, 1995.

[9] A. Arhrib, M. Capdequi–Peyranere, A. Djouadi, Phys. Rev. D52 (1995) 1404.

[10] J. Schwinger, Particles, Sources and Fields, Vol. II (Addison–Wesley, Reading, MA, 1970/73) Ch. 5.4.

[11] G. Passarino and M. Veltman, Nucl. Phys. B160 (1979) 151.

[12] A. Denner, Fortschr. Phys. 41 (1993) 307.

[13] D. Garcia, W. Hollik, R. A. Jiménez, J. Solà, Nucl. Phys. B427 (1994) 53;
R. A. Jiménez, J. Solà, UAB-FT-376, hep-ph/9511292.

[14] A. Sopczak, A. Bartl, W. Porod, H. Eberl, S. Kraml, W. Majerotto, Proceed. of the Workshop on Physics and Experiments with Linear Colliders, Morioka, Japan, 1995;
A. Bartl, H. Eberl, S. Kraml, W. Majerotto, W. Porod, A. Sopczak, Proceed. of the Workshop "Physics with e^+e^- Linear Colliders", Annecy–Gran Sasso–Hamburg, 1995.

Figure Captions

Fig. 1 Feynman diagrams for the lowest order SUSY–QCD corrections to $e^+e^- \to \tilde{q}_i\bar{\tilde{q}}_j$. Note that there are also the corresponding diagrams to c), d), e), h), and j) for the antisquark $\bar{\tilde{q}}_j$.

Fig. 2 SUSY–QCD corrections $\delta\sigma^g/\sigma^{tree}$ and $\delta\sigma^{\tilde{g}}/\sigma^{tree}$ as a function of $m_{\tilde{t}_1}$ for $e^+e^- \to \tilde{t}_1\bar{\tilde{t}}_1$ for $\sqrt{s} = 190$ GeV, $\cos\theta_{\tilde{t}} = 0.7$, $m_{\tilde{t}_2} = 250$ GeV, and $m_{\tilde{g}} = 200$ GeV.

Fig. 3 SUSY–QCD corrections $\delta\sigma^g/\sigma^{tree}$ and $\delta\sigma^{\tilde{g}}/\sigma^{tree}$ for $e^+e^- \to \tilde{t}_1\bar{\tilde{t}}_1$
(a) as a function of $\cos\theta_{\tilde{t}}$ for $\sqrt{s} = 500$ GeV, $m_{\tilde{t}_1} = 150$ GeV, $m_{\tilde{t}_2} = 300$ GeV, and $m_{\tilde{g}} = 300$ GeV,
(b) as a function of $\sqrt{s}$ for $\cos\theta_{\tilde{t}} = 0.7$, $m_{\tilde{t}_1} = 150$ GeV, $m_{\tilde{t}_2} = 300$ GeV, and $m_{\tilde{g}} = 300$ GeV.

Fig. 4 SUSY–QCD corrections $\delta\sigma^g$ and $\delta\sigma^{\tilde{g}}$ as a function of $\cos\theta_{\tilde{t}}$ for
$\sqrt{s} = 2$ TeV, $m_{\tilde{t}_1} = 500$ GeV, $m_{\tilde{t}_2} = 700$ GeV, and $m_{\tilde{g}} = 600$ GeV.
(a) for $e^+e^- \to \tilde{t}_1\bar{\tilde{t}}_1$
(b) for $e^+e^- \to \tilde{t}_1\bar{\tilde{t}}_2$
(c) for $e^+e^- \to \tilde{t}_2\bar{\tilde{t}}_2$

Fig. 5 Dependence of the SUSY–QCD corrections $\delta\sigma^g/\sigma^{tree}$ and $\delta\sigma^{g+\tilde{g}}/\sigma^{tree}$ on the gluino mass for $e^+e^- \to \tilde{t}_1\bar{\tilde{t}}_1$.
(a) for $\sqrt{s} = 500$ GeV, $m_{\tilde{t}_1} = 150$ GeV, $m_{\tilde{t}_2} = 300$ GeV, $\cos\theta_{\tilde{t}} = 0.5$
(b) for $\sqrt{s} = 2$ TeV, $m_{\tilde{t}_1} = 500$ GeV, $m_{\tilde{t}_2} = 700$ GeV, $\cos\theta_{\tilde{t}} = 0.5$

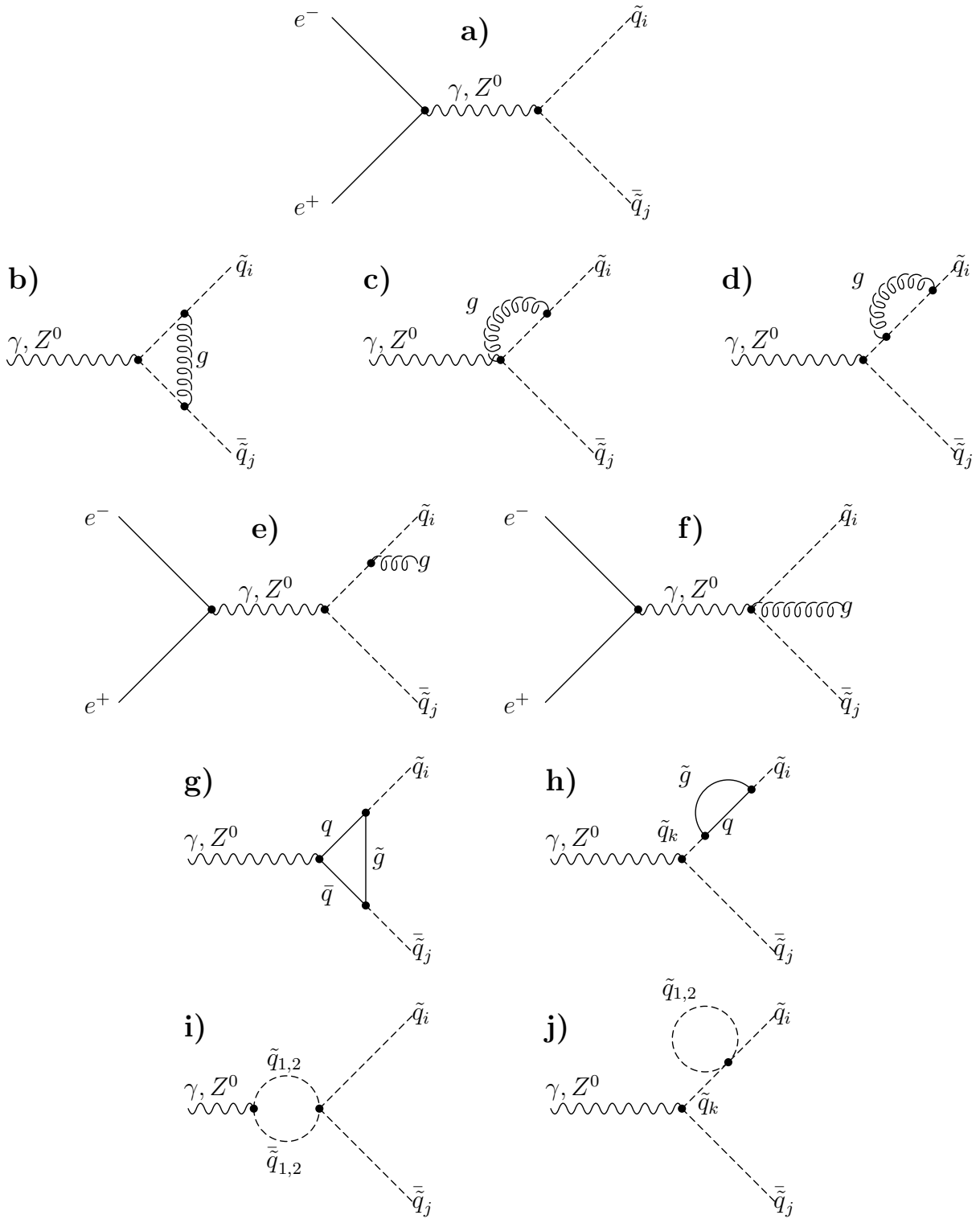
a)
e^-
e^+
γ, Z^0
$\tilde{q}_i$
$\bar{\tilde{q}}_j$
b)
c)
d)
g
e)
f)
g)
q
$\bar{q}$
$\tilde{g}$
h)
$\tilde{q}_k$
i)
$\tilde{q}_{1,2}$
$\bar{\tilde{q}}_{1,2}$
j)

Fig. 1

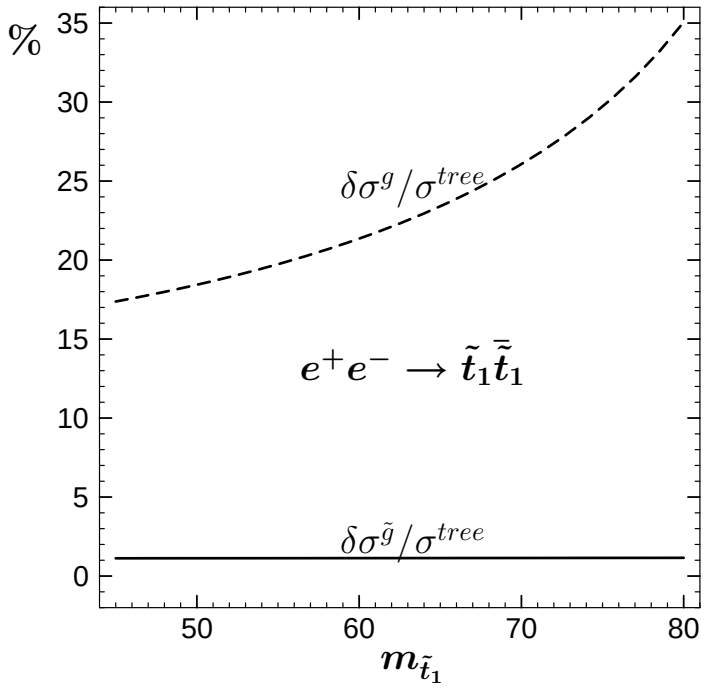
%
35
30
25
20
15
10
5
0
$\delta\sigma^g/\sigma^{tree}$
$e^+e^- \to \tilde{t}_1\bar{\tilde{t}}_1$
$\delta\sigma^{\tilde{g}}/\sigma^{tree}$
50
60
70
80
$m_{\tilde{t}_1}$

Fig. 2

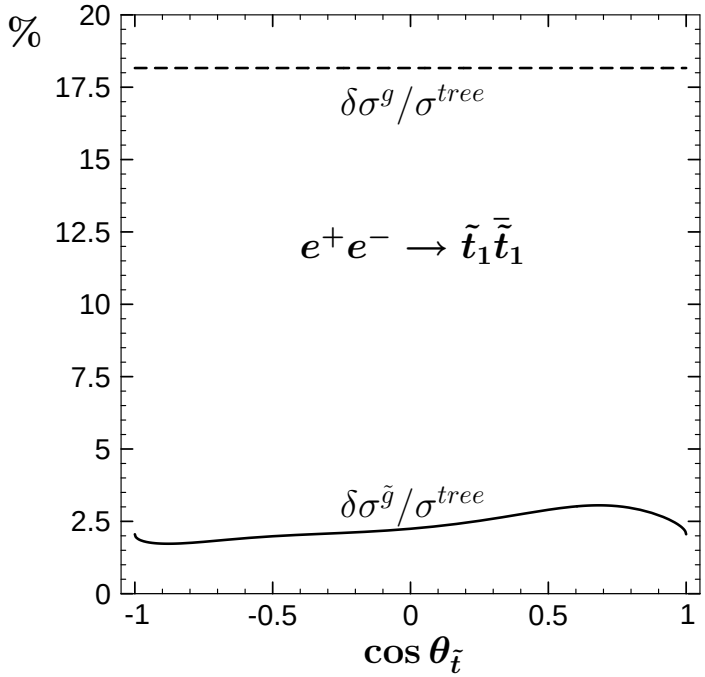
%
20
17.5
15
12.5
10
7.5
5
2.5
0
$\delta\sigma^g/\sigma^{tree}$
$e^+e^- \to \tilde{t}_1\bar{\tilde{t}}_1$
$\delta\sigma^{\tilde{g}}/\sigma^{tree}$
-1
-0.5
0
0.5
1
$\cos\theta_{\tilde{t}}$

Fig. 3a

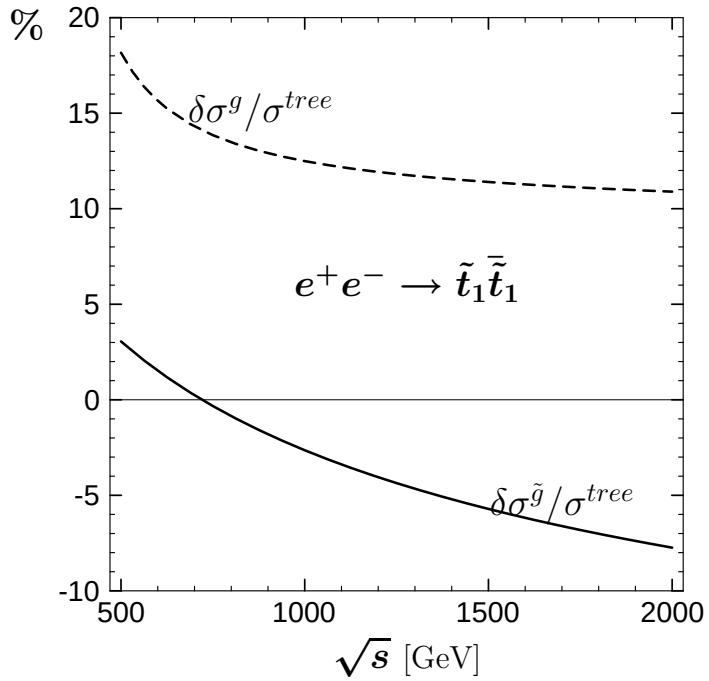
%
20
15
10
5
0
-5
-10
500
1000
1500
2000
$\delta\sigma^g/\sigma^{tree}$
$e^+e^- \to \tilde{t}_1\bar{\tilde{t}}_1$
$\delta\sigma^{\tilde{g}}/\sigma^{tree}$
$\sqrt{s}$ [GeV]

Fig. 3b

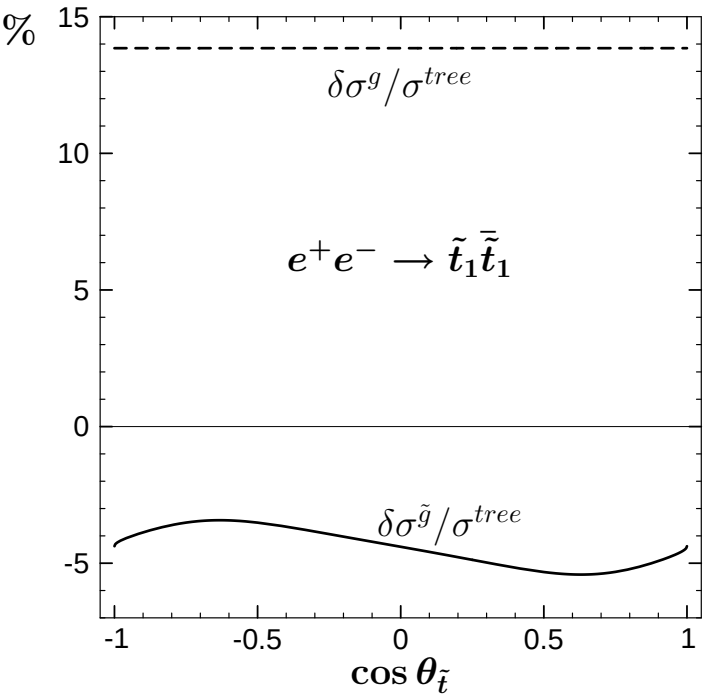
%
15
10
5
0
-5
-1
-0.5
0
0.5
1
$\delta\sigma^g/\sigma^{tree}$
$e^+e^- \to \tilde{t}_1\bar{\tilde{t}}_1$
$\delta\sigma^{\tilde{g}}/\sigma^{tree}$
$\cos\theta_{\tilde{t}}$

Fig. 4a

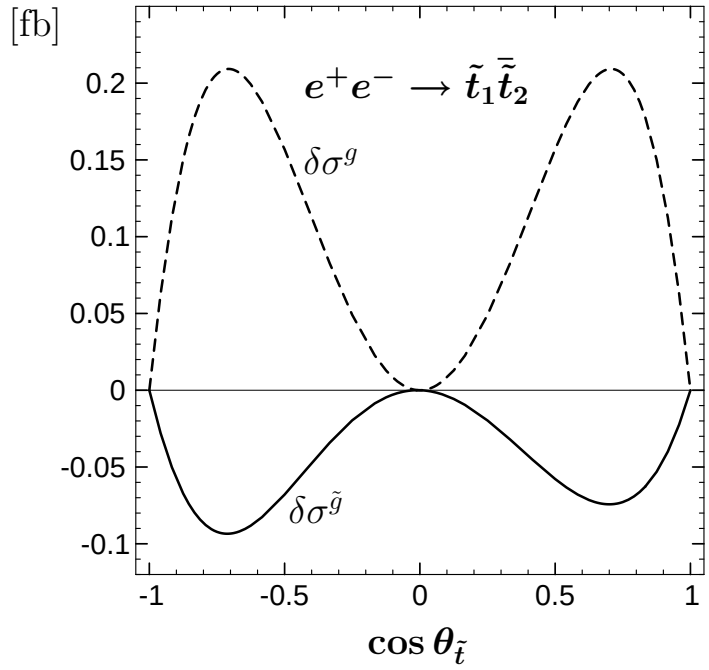
[fb]
$e^+e^- \to \tilde{t}_1\bar{\tilde{t}}_2$
$\delta\sigma^g$
$\delta\sigma^{\tilde{g}}$
0.2
0.15
0.1
0.05
0
-0.05
-0.1
-1
-0.5
0
0.5
1
$\cos\theta_{\tilde{t}}$

Fig. 4b

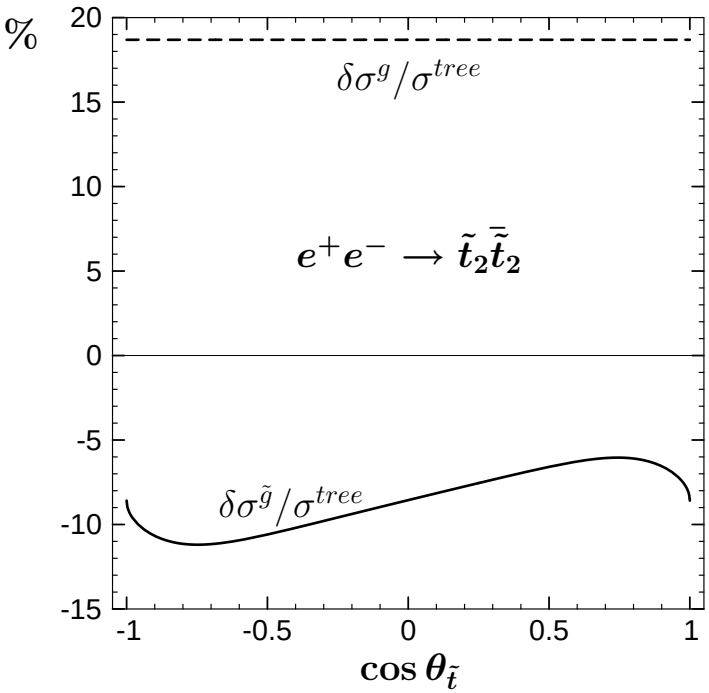
%
$\delta\sigma^g/\sigma^{tree}$
$e^+e^- \to \tilde{t}_2\bar{\tilde{t}}_2$
$\delta\sigma^{\tilde{g}}/\sigma^{tree}$
20
15
10
5
0
-5
-10
-15
-1
-0.5
0
0.5
1
$\cos\theta_{\tilde{t}}$

Fig. 4c

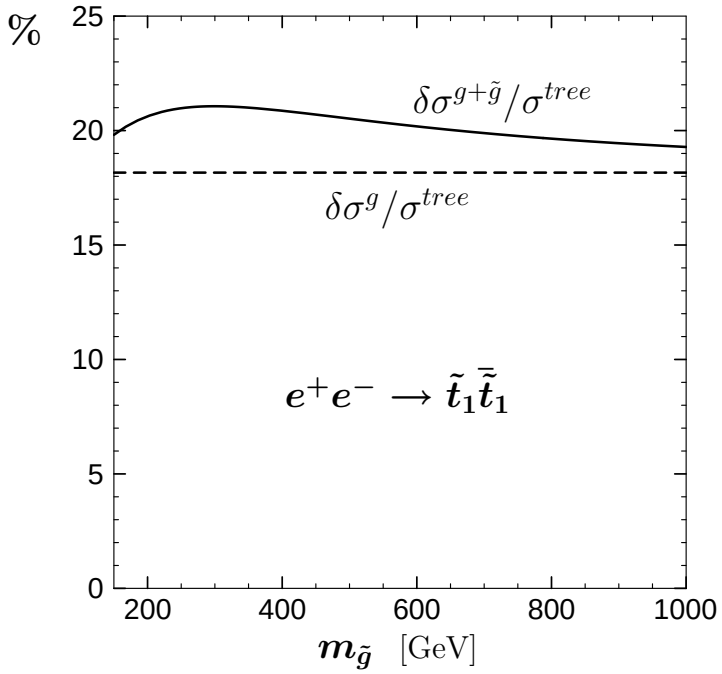
%
25
20
15
10
5
0
200
400
600
800
1000
$\delta\sigma^{g+\tilde{g}}/\sigma^{tree}$
$\delta\sigma^{g}/\sigma^{tree}$
$e^+e^- \to \tilde{t}_1\bar{\tilde{t}}_1$
$m_{\tilde{g}}$ [GeV]

Fig. 5a

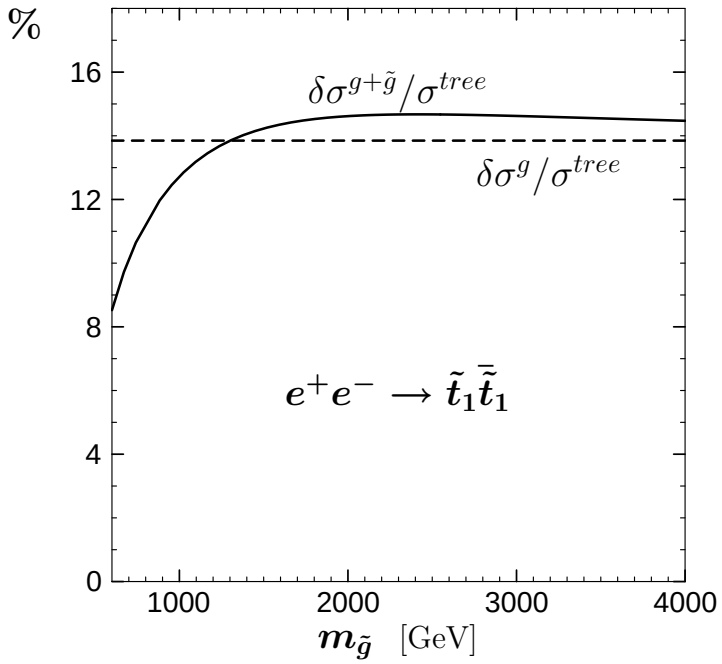
%
16
12
8
4
0
1000
2000
3000
4000
$\delta\sigma^{g+\tilde{g}}/\sigma^{tree}$
$\delta\sigma^{g}/\sigma^{tree}$
$e^+e^- \to \tilde{t}_1\bar{\tilde{t}}_1$
$m_{\tilde{g}}$ [GeV]

Fig. 5b